International Journal of GEOMATE, July, 2018 Vol.15, Issue 47, pp.81-88
Geotec., Const. Mat. & Env., DOI: https://doi.org/10.21660/2018.47.STR120
ISSN: 2186-2982 (Print), 2186-2990 (Online), Japan

NONLINEAR STRUT–AND–TIE MODEL WITH BOND–SLIP EFFECT FOR ANALYSIS OF RC BEAM–COLUMN JOINTS UNDER LATERAL LOADING

Rattapon Ketiyot[1], *Chayanon Hansapinyo[2] and Bhuddarak Charatpangoon[2]

[1] Department of Civil Engineering, Faculty of Engineering, Rajamangala University of Technology Lanna Chiang Rai Campus, Thailand;
[2] Center of Excellence for Natural Disaster Management, Department of Civil Engineering, Faculty of Engineering, Chiang Mai University, Thailand

*Corresponding Author, Received: 15 Feb. 2017, Revised: 16 Dec. 2017, Accepted: 30 Jan. 2018

ABSTRACT: This paper presents an application of nonlinear strut-and-tie model (NSTM) with bond-slip effect for analysis of reinforced concrete (RC) interior beam-column joints under lateral loading. The conventional STM is a calculation based on the force method exhibiting the internal forces in each component, it is unable to capture an inelastic response when RC beam-column joints undergo large displacement. Test results of three similar interior beam-column subassemblage frames with Grade400, Grade400s and Grade500 of longitudinal reinforcement bar, were used to verify the applicability of the NSTM, respectively. In the joint region, nonlinear links of concrete and steel bar with bond-slip effect were applied to simulate a load-displacement response. The results, such as maximum loading capacity, lateral load-story drift relation and failure mode, obtained from both NSTM models and laboratory experiments were compared. It was found that the results from the analyses using the NSTM with bond-slip effect agreed well with the experimental results. Furthermore, the demand-to-capacity ratios of the nonlinear links, which represents the distribution of the internal force in the NSTMs' joint region, exhibit the failure location and the failure mode that compatible with the experimental result. Hence, the proposed model is capable of predicting the strength of interior beam-column joint of RC frames under lateral loading.

Keywords: Nonlinear strut-and-tie model, Bond-slip effect, Interior beam-column joint, Lateral load

1. INTRODUCTION

During a large earthquake, the most critical region in the concrete moment resisting frame is the beam-column joint. The joint is subjected to a much higher shear force than other connected elements. The failure of the joint can lead to the brittle failure mode. Hence, force resisting mechanism of the joint is carefully considered for seismic action. A strut-and-tie model is the widely used joint model for estimating the joint capacity. It was first introduced by Park and Paulay [1] and provided in various design code provisions such as ACI318-14 [2] and NZS 3101-95 [3]. For the beam-column joint region of RC frames under lateral loading, the diagonal strut and reinforcements form truss mechanism that representing the transfer of shear force within the concrete joint, as shown in Fig. 1. Several researchers developed the joint model by considering a nonlinear behavior of concrete material. For example, Hwang and Lee [4] proposed a softened strut-and-tie model based on traditional strut- and- tie model according to ACI318-95 [5]. The proposed model was derived to satisfy equilibrium, compatibility, and the constitutive laws of cracked reinforced concrete. Similarly, Hong and Lee [6] presented the strut-and- tie model for RC beam- column joints to investigate the effect of shear strength degradation on the deformation of plastic hinges of adjacent beams. The bond stress distribution along the beam steel bars within the joint was considered in the study. Bonding behavior proposed by Soroushian *et al.* [7] was adopted for simulating the local bond slip of deformed bars in confined concrete.

In general, the conventional strut-and-tie model is a calculation based on the force method exhibiting the internal forces in each component. It is unable to capture an inelastic response when displacement becomes large. Chaimahawan and Pimanmas [8] proposed the use of nonlinear link with the strut-and-tie model for nonlinear analysis of existing reinforced concrete beam- column connection. The nonlinear links were provided in the critical region. The model was capable to predict the story shear and displacement relation. However, the large shear force in the joint also introduces bonding deterioration. Hence, this paper was aimed to present the applicability of the softened strut-and-tie model including bond-slip effect along longitudinal beam reinforcement within the concrete joint and plastic hinge region at column faces by using inelastic constitutive models from previous studies. The validity of the proposed model was examined by comparing the numerical results with the experimental results of three interior beam-column joint specimens.

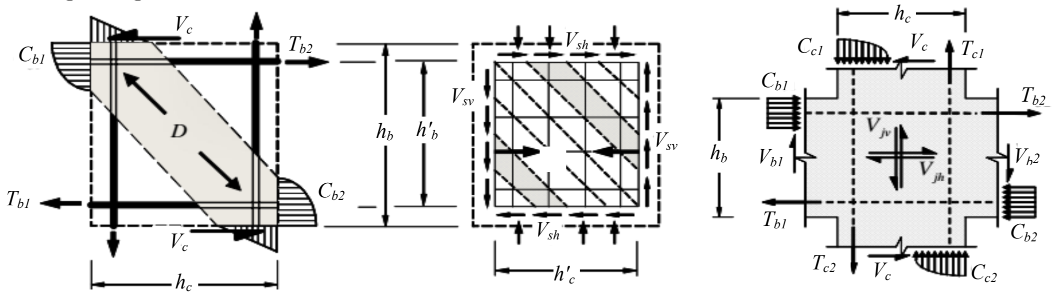

(a) Diagonal strut mechanism (b) Truss mechanism (c) Force acting on interior beam-column joint

Fig. 1 Shear mechanism of interior beam-column joint [4-5]

2. STUDY PROGRAM

In this study, test specimens and analytical models were classified according to the grade of longitudinal bars as shown in Table 1. Three grades of longitudinal bars were a conventional Grade 400 deformed rebar, a seismic Grade 400s bar with higher ductility, and a high strength Grade 500 bar.

Table 1 Test specimens and strut-and-tie model

Longitudinal bar grade	Test specimen	Analytical model
Grade 400	M-SD40-EXP	NSTM-SD40
Grade 400s	M-SD40s-EXP	NSTM-SD40s
Grade 500	M-SD50-EXP	NSTM-SD50

2.1 Experimental Program

The experimental study involved the test of the three 2/3 scaled cruciform shaped interior beam-column monolithic subassemblage frames having different grades of longitudinal reinforcement in each specimen. The test specimens were designed based on a seismic design philosophy according to ACI 318-14 and the ACI 352R-02 [9]. The identical reinforcement details were provided for all specimens, as shown in Fig. 2. A quasi-static lateral load (H) with a loading history according to ACI T1.1-01[10] was applied on the specimens by pushing forward and pulling backward the top of the upper column. Furthermore, a vertical axial load of $0.10f_c'A_g$ was constantly applied at the column tip.

2.2 Numerical Program

2.2.1 Generation of Strut-and-Tie model in the interior beam-column joint

Under high lateral load, the free body diagram of the interior beam-column joint along with its acting forces are shown in Fig. 1(c). The equilibrium of the horizontal forces on the joint of an RC frame can be explained in Eq. (1).

$$V_{jh} = T_{b1} + C_{b2} - V_c \tag{1}$$

where V_{jh} is the horizontal shear force in the joint; T_{b1} is the tensile force of the beam longitudinal reinforcement on a side of the column face; C_{b2} is the compressive force of beam on another side of the column face representing as beam flexural compression block; V_c is the column shear force that acting on the joint, equal to $[(M_{u1}+M_{u2})/h + (V_b h_c)/h]$; M_{u1} and M_{u2} ,as shown in Fig. 3, are the ultimate bending moment capacities of the two connecting beams; h is interstory height; V_b is the shear force in the beam; and h_c is the column depth in direction of the acting lateral force.

In equilibrium condition, the compressive stress, C_{b2}, is balanced with yielding force $T_{b2} = A_{s2}f_{y2}$. For the plastic yielding on another beam's end, T_{b1} is equal to $A_{s1}f_{y1}$. A_{s1} and A_{s2} are the cross sectional areas of tension reinforcement of the left (bottom) and right (top) side, respectively. The specified yield strength of the bottom and top reinforcement bars are represented as f_{y1} and f_{y2}, respectively. Hence, the Eq. (1) can be rewritten as shown in Eq. (2).

$$V_{jh} = A_{s1}f_{y1} + A_{s2}f_{y2} - \left(\frac{\left(M_{u1}+M_{u2}\right)}{h} + \frac{V_b h_c}{h}\right) \quad (2)$$

For a stress field within an interior beam-column joint shown in Fig. 4(a), the strut-and-tie model is developed in Fig. 4(b). The position of the internal tensile force (T_{b1}) in longitudinal bars is assumed to coincide with the resultant compression force (C_{b2}) in the compressive region of the beam section. Regarding strut angles of inclination α_1 and α_2, the calculation of the parameter can be expressed in Eqs. (3) - (4).

$$\tan\alpha_1 = \left(\frac{h_b'}{h_c'}\right) \quad (3)$$

$$\tan\alpha_2 = \left(\frac{h_b'}{2h_c'}\right) \quad (4)$$

where h_c' and h_b' are the distance between the longitudinal reinforcement in the column and beam, respectively. In order to calculate the flexural moment capacities (M_u) in Eq. (2) of the beam and column, the depths of beam and column in compression zone (a_b and a_c) is calculated as follows:

$$a_b = \frac{A_s f_y}{0.85 b_b f_c'} \quad (5)$$

$$a_c = \left(0.25 + \frac{N}{h_c b_c f_c'}\right) h_c \quad (6)$$

where A_s is the area of tensile steel bars of the beam; b_b and b_c are the beam width and column width, respectively; h_c is the thickness of column; and N is the axial load acting on the column.

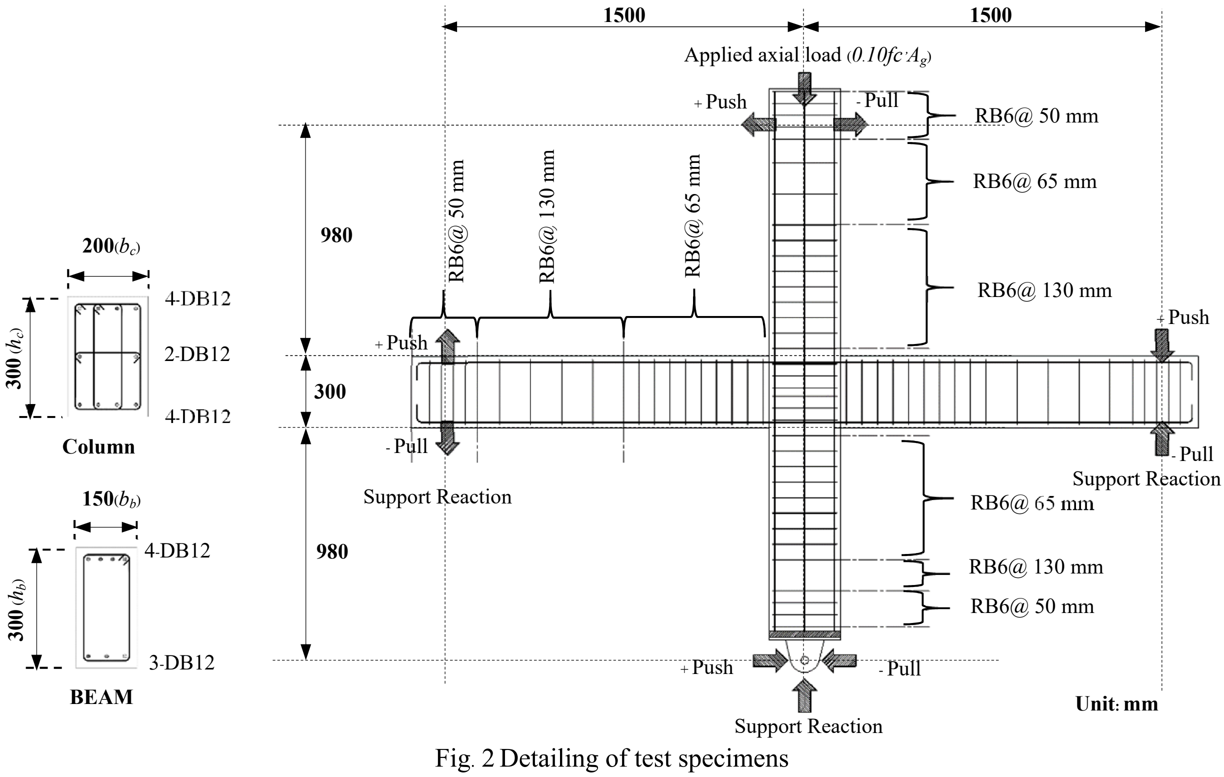

Fig. 2 Detailing of test specimens

2.2.2 Nonlinear Strut-and-tie model (NSTM)

To predict the maximum shear capacity of the test specimens, the NSTMs were generated by using CSI- SAP2000 software. Geometry and dimension of the NSTMs were given based on the test specimens. Linear strut- and- tie components were considered following ACI 318- 14. For the joint region and the plastic hinge region at beam-ends, nonlinear links were applied with nonlinear constitutive laws of specific materials. As shown in Fig. 5(a), the NSTM is composed of 90 linear components, 17 nonlinear link elements and 56 nodes. The nonlinear link elements are shown in Fig. 5(b). In this study, the NSTM was increasingly pushed at the column tip under laterally monotonic displacement.

2.3 Constitutive Law of Concrete and Reinforcing bar

In this study, the nonlinear links in the joint region were a relationship between load-displacement converted from constitutive stress-strain relations. For the nonlinear strut component, the compression loading is the multiplied result between compressive stress (σ_c) of the concrete model and the effective compressive area ($A_b = b_b$ x a_b and $A_c = b_c$ x a_c for strut components in beam and joint elements, respectively). The multiplied result of compressive strain (ε_c) and strut component length was used as the longitudinal displacement of the nonlinear struts. Similarly, in the nonlinear tie components, the tensile loading of the tie elements was the multiple of tensile stress (f_s) of steel bar and reinforcing area (A_s). Also, the multiplied result of the steel tensile stain (ε_s) and the tie length was used as the longitudinal displacement of the nonlinear tie components.

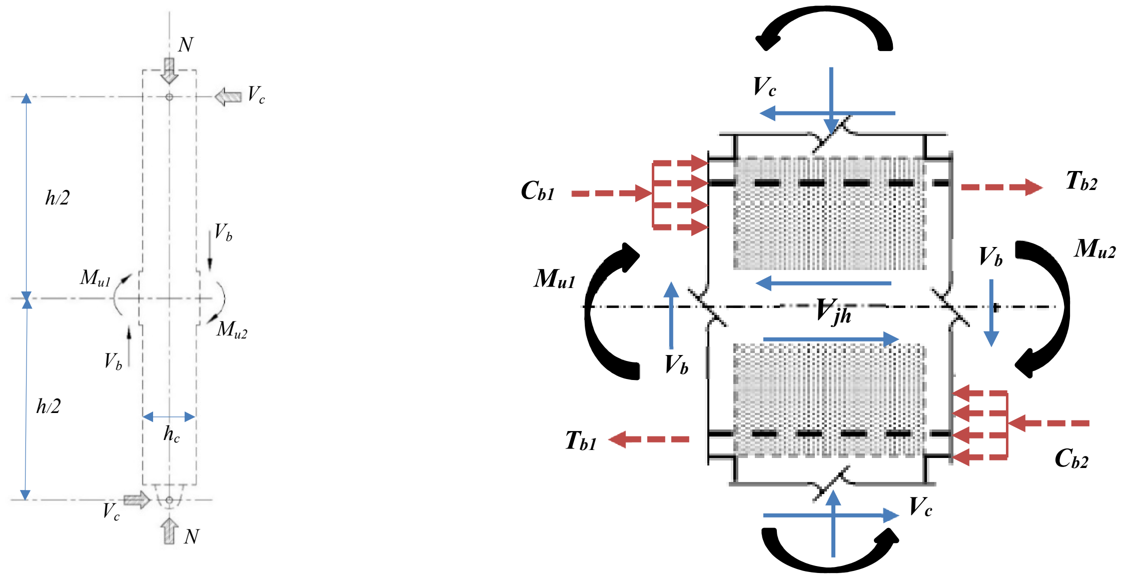

(a) Section of column (b) Section of joint

Fig. 3 Free body diagram of column and joint

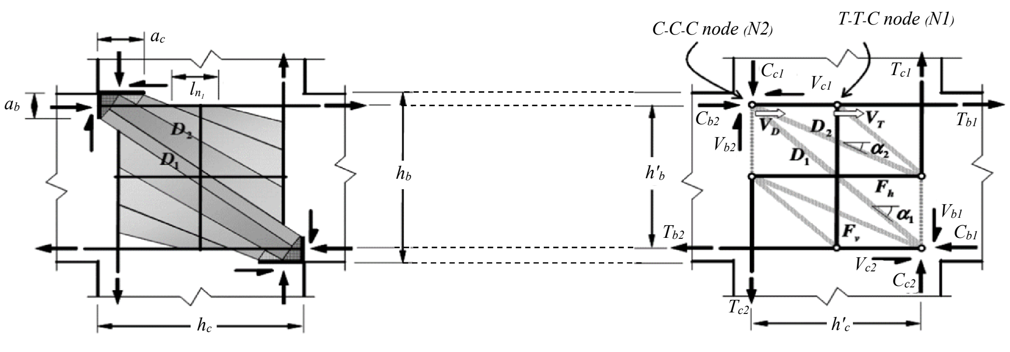

(a) Stress field within joint region (b) Strut-and-tie model within joint region

Fig. 4 Strut-and-tie model within beam-column interior joint region [4]

2.3.1 Softened concrete model for the nonlinear strut element

In this study, the nonlinear concrete model proposed by Maekawa *et al.* [11] was used to define the strut elements in the joint and plastic hinge region. The compressive strength and stiffness of concrete are reduced due to the occurrence of orthogonal tensile strain (ε_t) in term of a reduction factor (ω). For simplicity, the minimum reduction factor of 0.60, was assumed in this study. Fig. 6 shows the uniaxial constitutive law performed in the nonlinear spring of the strut-and-tie model. Only compression response was defined in the strut components. The uniaxial stress-strain relationship can be written as;

$$\sigma_c = \omega K_o E_{co} (\varepsilon - \varepsilon_p) \tag{7}$$

$$K_o = \exp\left(-0.73\frac{\varepsilon}{\varepsilon'}\left(1-\exp\left(-1.25\frac{\varepsilon}{\varepsilon'}\right)\right)\right) \tag{8}$$

$$\varepsilon_p = 2\varepsilon'\left(\frac{\varepsilon}{\varepsilon'}-\frac{20}{7}\left(1-\exp\left(-0.35\frac{\varepsilon}{\varepsilon'}\right)\right)\right) \tag{9}$$

where σ_c is the compressive stress parallel to crack direction; ω is strength reduction factor due to orthogonal tensile strain; K_o is the fracture parameter; E_{co} is the initial elastic modulus; ε_p is the compressive plastic strain; ε' is the strain at the peak compressive strength.

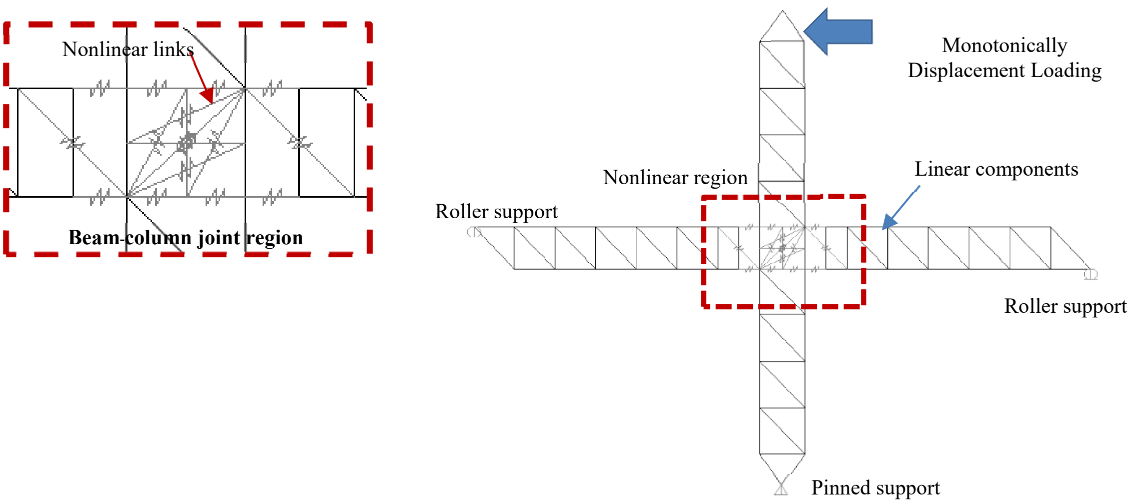

(a) Nonlinear strut-and-Tie model

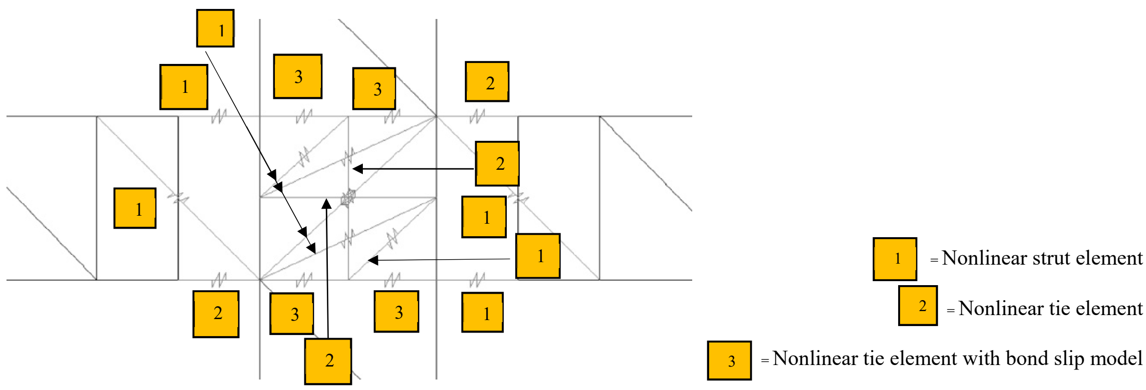

(b) Nonlinear links at the joint region

Fig. 5 Nonlinear strut-and-Tie model (NSTM) with nonlinear joint

2.3.2 Softened concrete model for the nonlinear strut element

In general, the stress-strain curve of the bare bar is assumed as an elasto-perfectly plastic. However, the stress-strain relationship of the bar embedded in the concrete structure is quite different. At crack sections, the embedded reinforcement behaves as the steel bar. Whilst, at the uncrack sections between the two consecutive crack sections, stress in the reinforcing bar is lower than the stress at the crack sections. A previous study of Hsu and Mo [12] proposed average or smeared reinforcing bar behavior between the crack and uncrack sections. Fig. 7 shows the smeared bilinear model of steel bar used in this study. The smeared yield stress of the bilinear model (f_y') was used to define the yield strength of the nonlinear tie elements.

2.4 Bond Behavior in the Joint Region

The bond- slip response in the joint was considered in the study. The bond-slip model was defined as the nonlinear link elements representing the longitudinal beam bars within the joint region in the NSTM, as shown in Fig. 5. The empirical equation of local bond stress and slip values proposed by Soroushian *et al.* [7] was adopted, as shown in Table 3 and Fig. 8.

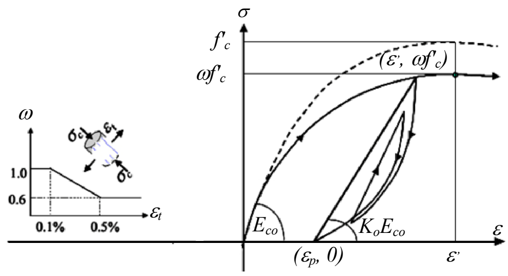

Fig. 6 Combined compression-tension model of concrete [11]

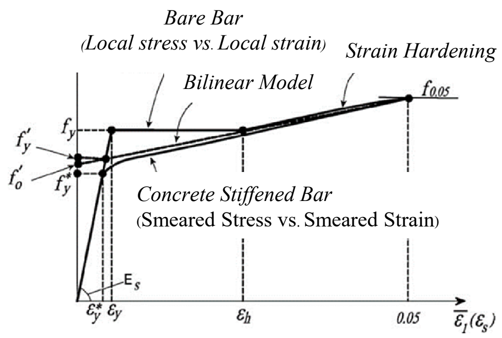

f_y = Yield strength of the bare bar
f_y* = Smeared yield stress of steel
f_y' = Smeared yield stress of the bilinear model
f_o' = Vertical intercept of the post-yield straight line
ε_y = Yield strain of bare bar
ε_y* = Smeared yield strain of steel

Fig. 7 Stress-strain relationship of steel bar [12]

Table 3 Empirical values for characteristic local bond stress and slip (Soroushian *et al.*)

τ_1 (MPa)	τ_3 (MPa)	S_1 (mm)	S_2 (mm)	S_3 (mm)
$\left(20-\frac{d_b}{4}\right)\sqrt{\frac{f'_c}{30}}$	5.00	1.00	3.00	10.50

where d_b is the bar diameter; S is bond slip; τ is bond stress; S_1, S_2 and S_3 are characteristic bond slip values for the local bond constitutive model, τ_1, τ_2 and τ_3 are characteristic bond stress values for the local bond constitutive model. τ_2 was assumed to equal to τ_1.

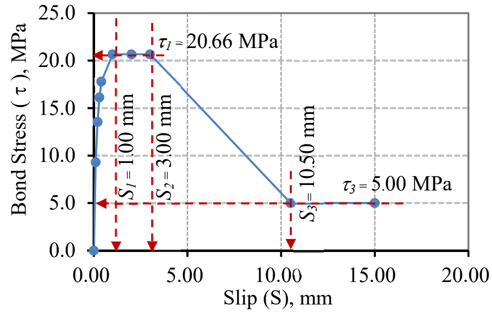

Fig. 8 Shape of local bond stress-slip model

3. RESULTS

3.1 Material properties

Concrete with the uniaxial compressive strength of 44.03 MPa was used to produce all specimens. The tensile mechanical properties of three grades of steel bars are shown in Table 4.

Table 4 Properties of longitudinal reinforcements

Grade of Steel Bar	Yield Strength, f_y (MPa)	Tensile Strength, f_u (MPa)	Elongation (%)
Grade 400	454	632	24.2
Grade 400s	468	568	28.5
Grade 500	560	716	20.3

Table 5 Strength and story drift level at peak of story shear

Specimen	Push (H+)/ Pull (H-)		Average capacity, H_{EXP} (kN)
	Ultimate Load (kN)	Corresponding Story Drift (%)	
M-SD40-EXP	44.43/42.08	2.00/3.50	43.25
M-SD40s-EXP	44.03/44.24	2.00/2.50	44.14
M-SD50-EXP	48.48/48.09	2.00/2.50	48.28

3.2 Experimental result

Fig. 9 shows the load-displacement hysteresis response of all test specimens. The ultimate load capacities of test specimens are shown in Table 5.

3.3 Numerical Results with the NSTM

Fig. 9 shows the monotonically backbone curves of NSTMs along with the enveloped curves obtained from the experimental results. It can be seen that both results are in good agreement. The maximum capacities of the NSTMs are shown in Table 6. The comparisons revealed that the NSTMs accurately predicted the ultimate capacity; and relation between the lateral story shear and the lateral displacement. Table 7 shows the maximum loading capacities of the analyzed frames using NSTM (H_{NSTM}), experimental results (H_{EXP}) and calculated values from ACI318-14 design code (H_{CAL}).

Table 6 Strength and story drift level at peak of story shear

NSTM Model	Numerical Result	
	Maximum Load, H_{NSTM} (kN)	Corresponding Story Drift (%)
NSTM-SD40	47.99	1.62
NSTM-SD40s	46.21	1.85
NSTM-SD50	51.30	1.78

Table 7 Strength and story drift level at peak of story shear

Series	H_{EXP} (kN)	H_{CAL} (kN)	H_{NSTM} (kN)	H_{NSTM} /H_{CAL}	H_{CAL} /H_{EXP}	H_{NSTM} /H_{EXP}
M-SD40	43.25	42.44	47.99	1.13	0.98	1.11
M-SD40s	44.14	40.30	46.21	1.15	0.91	1.05
M-SD50	48.28	45.33	51.30	1.13	0.94	1.06
Average				1.14	0.94	1.07

Regarding the internal force in the joint region of the NSTMs, Fig. 10 shows demand-to-capacity ratio (D/C ratio) of the strut- and- tie elements. The NSTM-SD40 and NSTM-SD40s models are very similar in terms of the force distribution, the failure location and the failure mode. The D/C ratios of the tie-link element representing the steel bar at the column face are equal to 1.00 as shown in Figs. 10 (a-b), meaning that the stress of the bar was reached to the yield level. For the specimen NSTM-SD50, the D/C ratios of the strut-link element representing the compressive portion of the concrete section at the column face are equal to 1.00. This indicates the compression failure of concrete which is similar to the failure mode obtained from the experimental result of specimen M-SD50.

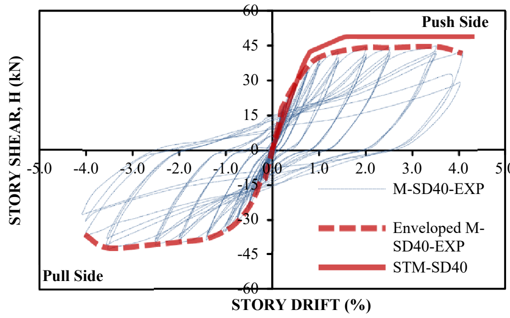

a) Story shear force vs. story drift ratio of M-SD40 series

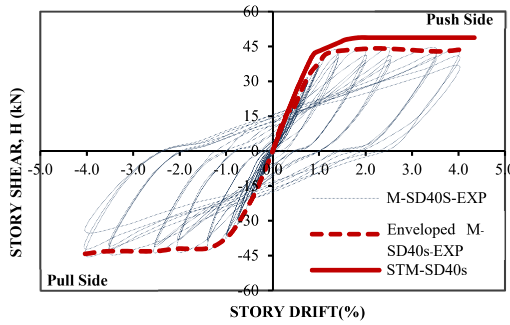

b) Story shear force vs. story drift ratio of M-SD40s series

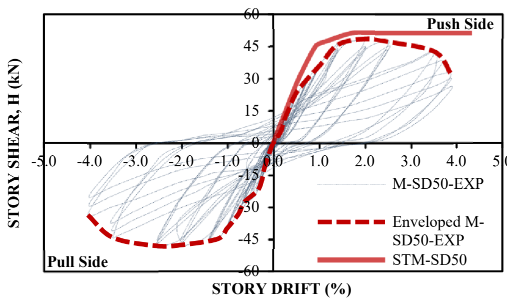

c) Story shear force vs. story drift ratio of M-SD50 series

Fig. 9 Experimental and numerical results

4. CONCLUSIONS

This paper presents the test and analysis of RC subassemblies under lateral loading. Nonlinear strut-and-tie model with bond-slip effect in the joint region were adopted in the analysis. The numerical results from the NSTMs such as maximum loading capacity, lateral load-story drift relation and failure mode were verified to the experimental results. The results from the analyses with the NSTMs agreed well with the experimental results. The ultimate lateral load from the analyses, experiments and ACI318-14 are all similar. Modes of failure of all NSTMs are compatible with the failure mode in the experimental results. Hence, it can be said that the analysis using the nonlinear strut-and-tie model with bond-slip effect in the joint zone is capable of predicting the ultimate capacity of RC frames under lateral loading.

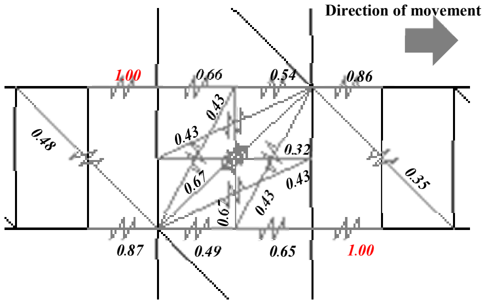

a) NSTM-SD40

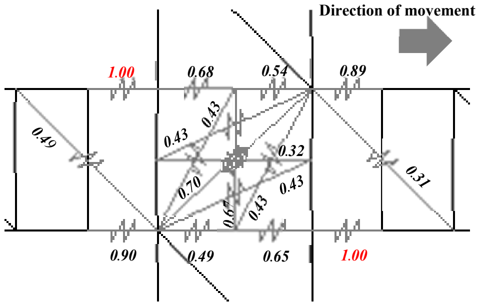

b) NSTM-SD40s

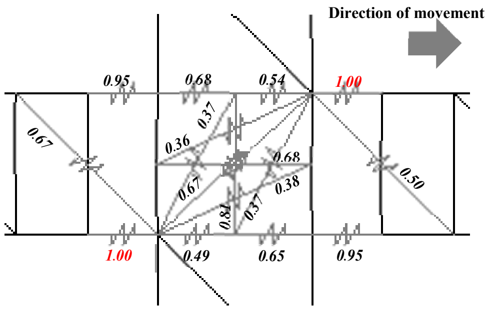

c) NSTM-SD50

Fig. 10 Demand to capacity ratio at joint region of NSTMs

5. REFERENCES

[1] Park R. and Pauley T. , Reinforced Concrete Structures, New York: John Wiley and Sons, 1975.

[2] American Concrete Institute, ACI 318-14: Building Code Requirements for Structural Concrete, Farmington Hills: MI, 2014.

[3] NZS 3101, Concrete Structures Standard NZS 3101: Part 1, Commentary NZS 3101: Part 2, Standards Association of New Zealand, Wellington: New Zealand, 1995.

[4] Hwang S.J. and Lee H.J., Analytical Model for Predicting Shear Strength of Interior Reinforced Concrete Beam- Column Joints for Seismic Resistance, ACI Structural Journal, Vol. 97, Issue 1, 2000, pp. 35-44.

[5] American Concrete Institute, ACI 318-95: Building Code Requirements for Structural Concrete, Farmington Hills, MI, 1995.

[6] Hong S.G. and Lee S.G., Strut-and-Tie Models for Deformation of Reinforced Concrete Beam-Column Joints dependent on Plastic Hinge Behavior of Beams, In Proc. 13th World Conference on Earthquake Engineering, 2004, pp. 1-6.

[7] Soroushian P., Choi K.B., Park G.H. and Aslani F., Bond of Deformed Bars to Concrete: Effects of Confinement and Strength of Concrete, Materials Journal, Vol. 88, Issue 3, 1991, pp. 227-232.

[8] Chaimahawan P. and Pimanmas A., Application of Nonlinear Link In Strut and Tie Model for Joint Planar Expansion, EIT Research and Development Journal, Vol. 24, Issue 4, 2013, pp.1-11.

[9] American Concrete Institute, ACI 352R- 02: Recommendations for Design of Beam- Column Connection in Monolithic Reinforced Concrete Structures by ACI- ASCE Committee 352, Farmington Hills, MI, 2002.

[10] American Concrete Institute, ACI T1. 1- 01: Acceptance Criteria for Moment Frames Based on Structural Testing, Farmington Hills, MI, 2001.

[11] Maekawa K., Okamura H. and Pimanmas A. Non-linear Mechanics of Reinforced Concrete, New York, CRC Press, 2003.

[12] Hsu T.T. and Mo Y.L., Unified Theory of Concrete Structures, New York, John Wiley and Sons, 2010.